Hindawi Publishing Corporation
Advances in Mathematical Physics
Volume 2014, Article ID 538950, 9 pages
http://dx.doi.org/10.1155/2014/538950

Research Article

Effect of Velocity Slip Boundary Condition on the Flow and Heat Transfer of Cu-Water and TiO_2-Water Nanofluids in the Presence of a Magnetic Field

Abdelhalim Ebaid,[1] Fahd Al Mutairi,[2] and S. M. Khaled[3,4]

[1] *Department of Mathematics, Faculty of Science, University of Tabuk, P.O. Box 741, Tabuk 71491, Saudi Arabia*
[2] *Department of Chemical Engineering, Faculty of Engineering, University of Tabuk, Tabuk, Saudi Arabia*
[3] *Department of Mathematics, Faculty of Sciences, Helwan University, Cairo, Egypt*
[4] *Department of Studies and Basic Sciences, Faculty of Community, University of Tabuk, Tabuk, Saudi Arabia*

Correspondence should be addressed to Abdelhalim Ebaid; aebaid@ut.edu.sa

Received 24 April 2014; Revised 21 May 2014; Accepted 26 June 2014; Published 5 August 2014

Academic Editor: Ricardo Weder

In nanofluid mechanics, it has been proven recently that the no slip condition at the boundary is no longer valid which is the reason that we consider the effect of such slip condition on the flow and heat transfer of two types of nanofluids. The present paper considers the effect of the velocity slip condition on the flow and heat transfer of the Cu-water and the TiO_2-water nanofluids over stretching/shrinking sheets in the presence of a magnetic field. The exact expression for the fluid velocity is obtained in terms of the exponential function, while an effective analytical procedure is suggested and successfully applied to obtain the exact temperature in terms of the generalized incomplete gamma function. It is found in this paper that the Cu-water nanofluid is slower than the TiO_2-water nanofluid for both cases of the stretching/shrinking sheets. However, the temperature of the Cu-water nanofluid is always higher than the temperature of the TiO_2-water nanofluid. In the case of shrinking sheet the dual solutions have been obtained at particular values of the physical parameters. In addition, the effect of various physical parameters on such dual solutions is discussed through the graphs.

1. Introduction

Nanofluids are base fluids containing suspended nanoparticles. These nanoparticles are typically made of metals, oxides, carbides, or carbon nanotubes. The common base fluids include water, ethylene glycol, toluene, and oil. In the recent times, the study of nanofluid flow over a stretching sheet has gained much interest because of its numerous industrial applications. A few of these applications in engineering are polymer extrusion, wire drawing, continuous casting, manufacturing of foods and paper, glass fiber production, stretching of plastic films, glass blowing, manufacturing of plastic and rubber sheets, crystal growing, and continuous cooling and fiber spinning [1] and stretching of plastic films. In particular, during the manufacture of these sheets, the melt issues from a slit and is subsequently stretched to achieve the desired thickness. Hence, the final product with the desired characteristics strictly depends upon the stretching rate, the rate of cooling in the process, and the process of stretching [2]. Therefore, the choice of a proper cooling/heating liquid is essential as it has a direct impact on the rate of heat transfer. In addition, nanomaterials are of great interest in biology and medicine, owing to their numerous applications including DNA/protein detection, biomolecular regulators, cell imaging, and cancer cell diagnostics. Currently, the use of nanomaterials as drug delivery systems has become an emerging area in the field of nanomedicine. A wide variety of nanomaterials, such as nanotubes, nanorods, and nanoparticles, have been explored as carriers for delivering small molecule drugs, proteins, and genetic materials, exploiting their unique dimensions and specific physical and chemical properties [3].

Choi [4] may be the first author to introduce the word nanofluid that represents the fluid in which nanoscale particles (diameter < 50 nm) are suspended in the base fluid. The common nanoparticles that have been used are Aluminum, Copper, Silver, and Titanium or their oxides. Convective heat transfer of such nanoparticles in a base fluid is a topic of major interest both in applied sciences and engineering, where a very good review was presented by Saidur et al. [5] and Wang and Mujumdar [6, 7]. In this field, recent researches showed that nanoparticles changed the fluid characteristics because thermal conductivity of these particles was higher than convectional fluids. It was showed experimentally by Eastman et al. [8] and Xuan and Li [9] that the thermal conductivity of the base liquid can be enhanced by 10–20% with adding a small volumetric fraction of nanoparticles (usually < 5%). The enhanced thermal conductivity of nanofluids contributes to a remarkable improvement in the convective heat transfer coefficient. Recently, Hamad [10] studied the boundary-layer and heat transfer of nanofluids over impermeable isothermal stretching sheet for the metallic and metallic oxide nanoparticles. Noghrehabadi et al. [11] analyzed the heat transfer enhancement of water in the presence of SiO_2 nanoparticles over an isothermal stretching sheet. In addition, Noghrehabadi et al. [12] examined theoretically the flow and heat transfer of two types of nanofluids, namely Silver-water and Silicon Dioxide-water. They solved the governing equations by applying a combination of a symbolic power series and Padé approximation method. Further, Vajravelu et al. [13] studied the effect of variable viscosity on the flow and heat transfer of a viscous Ag-water and Cu-water nanofluids. They indicated that nanoparticle volume fraction is to increase the heat transfer and hence enhance the thermal boundary layer thickness. Moreover, an analysis has been performed by Alegn et al. [14] to study the heat transfer characteristics of steady two-dimensional boundary layer flow past a moving permeable flat plate in an alumina-water nanofluid. They have indicated that suction delays the boundary layer separation, while injection accelerates it.

In [15], Das has investigated numerically the mixed convection stagnation point flow and heat transfer of Cu-water nanofluids impinging normally towards a shrinking sheet. Very recently, Aly and Ebaid [16] introduced a direct and effective approach to obtain the exact analytical solution for the nanoparticles-water flow over an isothermal stretching sheet with effect of the slip model. In particular, they examined and compared the effect of existence of five metallic and nonmetallic nanoparticles, namely, Silver, Copper, Alumina, Titania, and Silicon Dioxide, in a base of water. They introduced a very direct and effective approach to analytically obtain the exact solution which was found in a very good agreement with the previous published results.

It has been shown in [17] that nanofluidic flow usually exhibits partial slip against the solid surface, which can be characterized by the so-called slip length (around 3.4–68 mm for different liquids). Accordingly, the authors in [18] discussed the effect of partial slip boundary condition on the flow and heat transfer of nanofluids past stretching sheet at constant wall temperature. Furthermore, the no-slip condition is no longer valid for fluid flows at the micro and nano scale and, instead, a certain degree of tangential slip must be allowed (see [19, 20]).

Due to importance of the slip effect on modeling the boundary layer flows of nanofluids, a theoretical investigation has been introduced in this paper for studying the effect of the velocity slip boundary condition on the flow and heat transfer of Cu-water and TiO_2-water nanofluids over a linearly stretching/shrinking sheets in the presence of magnetic field. Moreover, we introduce a direct and effective approach to analytically obtain the exact solutions for the governing nonlinear differential equation of the flow in terms of the exponential function while the temperature equation is solved exactly in terms of the generalized incomplete gamma function. The dual solutions have been also obtained in the case of the shrinking sheet. Further, we discuss the interested physical quantities, for example, the velocity and temperature, with comparison to results in literature. The structure of the paper is as follows. Description of the problem and basic equations are presented in Section 2. In Section 3, the exact analytical solutions of the flow and the temperature distribution are presented. In Section 4, we present the obtained numerical results. We finally conclude our paper in Section 5.

2. Basic Equations

Here, we consider a laminar steady two-dimensional incompressible viscous nanofluid over linearly semi-infinite stretching/shrinking sheets. A constant magnetic field is applied normally to the sheet. The fluid is a water-based nanofluid containing two different volume fractions of the Copper (Cu) and the Titania (TiO_2) nanoparticles. The thermophysical properties of the base fluid and nanoparticles are given (see Table 1 in [21]). The governing boundary-layer equations of the considered nanofluid can be written in the following form [10]:

$$\begin{aligned} &f'''(\eta) + (1-\phi)^{2.5}\left[1-\phi+\phi\left(\frac{\rho_s}{\rho_f}\right)\right] \\ &\quad\cdot\left[f(\eta)f''(\eta) - \left(f'(\eta)\right)^2\right] \\ &\quad - M(1-\phi)^{2.5}f'(\eta) = 0, \\ &\frac{1}{\Pr}\left(\frac{k_{nf}}{k_f}\right)\frac{1}{\left[1-\phi+\phi\left(\rho C_p\right)_s/\left(\rho C_p\right)_f\right]} \\ &\quad\cdot\theta''(\eta) + f(\eta)\theta'(\eta) = 0, \end{aligned} \tag{1}$$

where primes denote the differentiation with respect to a similarity variable η, $f(\eta)$ and $\theta(\eta)$ are the dimensionless stream function and temperature, respectively, ϕ is the solid volume fraction, ρ_f and ρ_s are the densities, $(\rho C_p)_f$ and $(\rho C_p)_s$ are the heat capacitances, M is the magnetic parameter, Pr is the Prandtl number, and k_{nf} is the thermal conductivity defined as follows [22, 23]:

$$\frac{k_{nf}}{k_f} = \frac{\left(k_s+2k_f\right) - 2\phi\left(k_f-k_s\right)}{\left(k_s+2k_f\right) + \phi\left(k_f-k_s\right)}, \tag{2}$$

where k_f and k_s are the thermal conductivities, where $()_f$ and $()_s$ denote the basic fluid and solid fractions, respectively. The flow is subjected to the boundary conditions:

$$\begin{gathered} f(0) = 0, \\ f'(0) = 1 + \lambda f''(0), \\ f'(\infty) = 0, \\ (\text{Stretching sheet}), \\ f(0) = s(>0), \\ f'(0) = -1 + \lambda f''(0), \\ f'(\infty) = 0, \\ (\text{Shrinking sheet}) \end{gathered} \tag{3}$$

$$\begin{gathered} \theta(0) = 1, \\ \theta(\infty) = 0, \end{gathered} \tag{4}$$

where λ is a slip parameter. Equations (1) can be rewritten as

$$f'''(\eta) + \alpha\left[f(\eta) f''(\eta) - \left(f'(\eta)\right)^2\right] - \gamma f'(\eta) = 0, \tag{5}$$

$$\tau\theta''(\eta) + f(\eta)\theta'(\eta) = 0, \tag{6}$$

where

$$\begin{aligned} \alpha &= (1-\phi)^{2.5}\left[1 - \phi + \phi\left(\frac{\rho_s}{\rho_f}\right)\right], \\ \gamma &= M(1-\phi)^{2.5}, \\ \tau &= \frac{1}{\Pr}\left(\frac{k_{nf}}{k_f}\right)\frac{1}{\left[1 - \phi + \phi\left(\rho C_p\right)_s / \left(\rho C_p\right)_f\right]}. \end{aligned} \tag{7}$$

In the case of the stretching sheet, it should be noted that the first part of the current paper reduces to Hamad [10] in the absence of the slip effect; that is, $\lambda = 0$.

3. Exact Solutions

In this section, an effective analytical procedure shall be presented to exactly solve the system (5)-(6) with the boundary conditions (3)-(4) for both cases of the stretching and the shrinking sheets. In this regard, we observe from (5) that only unknown $f(\eta)$ is involved which is the reason that we begin with solving this f-differential equation in the next section.

3.1. Stretching Sheet

3.1.1. Exact Solution for the Stream Function $f(\eta)$. In view of the boundary conditions given in (3), it is reasonable to assume $f(\eta)$ in the form:

$$f(\eta) = a + be^{-\beta\eta}, \tag{8}$$

in which the infinity boundary condition is automatically satisfied provided that $\beta > 0$. On using (8) into (5), we have

$$\beta b\left(\beta^2 - \alpha a\beta - \gamma\right)e^{-\beta\eta} = 0, \tag{9}$$

which leads to

$$\beta^2 - \alpha a\beta - \gamma = 0. \tag{10}$$

Applying the first two boundary conditions given in (2), we obtain

$$\begin{gathered} a + b = 0, \\ \lambda b\beta^2 + b\beta + 1 = 0. \end{gathered} \tag{11}$$

Solving the system of the algebraic equations (10)-(11) for a, b, and β, we obtain

$$\begin{aligned} a &= \frac{1}{\beta(\lambda\beta + 1)}, \\ b &= -\frac{1}{\beta(\lambda\beta + 1)}, \end{aligned} \tag{12}$$

where β satisfies the following cubic algebraic equation:

$$\lambda\beta^3 + \beta^2 - \gamma\lambda\beta - (\alpha + \gamma) = 0. \tag{13}$$

It is also important here to refer to the fact that β is a positive real root of (13). Moreover, the exact solution given by (8) with a, b, and β given in (12) and (13) can be checked by direct substituting. Further, in the case of no slip, that is, $\lambda = 0$, $f(\eta)$ reduces to that obtained by [10] (given by (14)-(15)). Regarding the heat transfer equation, we shall discuss in the next section an effective analytical procedure for obtaining the exact solution in terms of the generalized incomplete gamma function.

3.1.2. Exact Solution of the Heat Transfer $\theta(\eta)$. In order to solve the heat transfer equation, we first use (8) to rewrite (6) in terms of only $\theta(\eta)$ as

$$\tau\theta''(\eta) + \left(a + be^{-\beta\eta}\right)\theta'(\eta) = 0. \tag{14}$$

On using separation technique and performing the integration once with respect to η from 0 to η, yields

$$\theta'(\eta) = \theta'(0)\, e^{-(a/\tau)\eta + (b/\tau\beta)e^{-\beta\eta} - (b/\tau\beta)}. \tag{15}$$

Integrating (15) once again with respect to η from 0 to η, we obtain

$$\theta(\eta) = \theta(0) + \theta'(0)\int_0^\eta e^{-(a/\tau)\sigma + (b/\tau\beta)e^{-\beta\sigma} - (b/\tau\beta)}\, d\sigma. \tag{16}$$

In view of the first condition in (4), we have

$$\theta(\eta) = 1 + \theta'(0)\, e^{-b/\tau\beta}\int_0^\eta e^{-(a/\tau)\sigma + (b/\tau\beta)e^{-\beta\sigma}}\, d\sigma. \tag{17}$$

The integration in the right-hand side can be analytically solved in terms of a well-known special function as declared by the following procedure. We first suppose that

$$\mu = -\frac{b}{\tau\beta} e^{-\beta\sigma}. \tag{18}$$

Accordingly

$$\begin{aligned} d\sigma &= -\frac{d\mu}{\beta b \mu}, \\ e^{-\sigma} &= \left(-\frac{\tau\beta}{b}\right)^{1/\beta} \mu^{1/\beta}. \end{aligned} \tag{19}$$

Inserting (18) and (19) into (17) gives

$$\begin{aligned} \theta(\eta) = 1 &+ \frac{1}{\beta b}\left(-\frac{\tau\beta}{b}\right)^{a/\tau\beta} \theta'(0)\, e^{-b/\tau\beta} \\ &\cdot \int_{-(b/\tau\beta)e^{-\beta\eta}}^{-b/\tau\beta} \mu^{(a/\tau\beta)-1} e^{-\mu} d\mu. \end{aligned} \tag{20}$$

On using the definition of the generalized incomplete gamma function,

$$\Gamma(c, z_0, z_1) = \int_{z_0}^{z_1} \mu^{c-1} e^{-\mu} d\mu, \tag{21}$$

we can rewrite (20) as

$$\begin{aligned} \theta(\eta) = 1 &+ \frac{1}{\beta b}\left(-\frac{\tau\beta}{b}\right)^{a/\tau\beta} \theta'(0)\, e^{-b/\tau\beta} \\ &\cdot \Gamma\left(\frac{a}{\tau\beta}, -\frac{b}{\tau\beta} e^{-\beta\eta}, -\frac{b}{\tau\beta}\right). \end{aligned} \tag{22}$$

Imposing the boundary condition $\theta(\infty) = 0$, we obtain the following explicit value for $\theta'(0)$:

$$\theta'(0) = \frac{-\beta b(-\tau\beta/b)^{-a/\tau\beta} e^{b/\tau\beta}}{\Gamma(a/\tau\beta, 0, -b/\tau\beta)}. \tag{23}$$

Inserting this value of $\theta'(0)$ into (22), we get

$$\theta(\eta) = 1 - \frac{\Gamma\left(a/\tau\beta, -(b/\tau\beta)\, e^{-\beta\eta}, -b/\tau\beta\right)}{\Gamma(a/\tau\beta, 0, -b/\tau\beta)}. \tag{24}$$

This expression for $\theta(\eta)$ can be further simplified by using the following identity for the generalized incomplete gamma function:

$$\Gamma(c, 0, z_1) - \Gamma(c, z_0, z_1) = \Gamma(c, 0, z_0). \tag{25}$$

Hence, the exact solution for the temperature distribution $\theta(\eta)$ is finally given by

$$\theta(\eta) = \frac{\Gamma\left(a/\tau\beta, 0, -(b/\tau\beta)\, e^{-\beta\eta}\right)}{\Gamma(a/\tau\beta, 0, -b/\tau\beta)}. \tag{26}$$

3.2. Shrinking Sheet. Following the same analysis as in the stretching sheet we can get the velocity exact solution as

$$f(\eta) = c + d e^{-\delta\eta}, \tag{27}$$

in which the infinity boundary condition is automatically satisfied provided that $\delta > 0$, where c and d are given by

$$\begin{aligned} c &= s - \frac{1}{\delta(\lambda\delta + 1)}, \\ d &= \frac{1}{\delta(\lambda\delta + 1)}, \end{aligned} \tag{28}$$

and δ should be at least one positive root of the cubic algebraic equation:

$$\lambda\delta^3 + (1 - \alpha\lambda s)\,\delta^2 - (\alpha s + \gamma\lambda)\,\delta + (\alpha - \gamma) = 0. \tag{29}$$

The temperature distribution is given by the same formula in the case of the stretching sheet with replacing a by c, replacing b by d, and replacing β by δ; that is,

$$\theta(\eta) = \frac{\Gamma\left(c/\tau\delta, 0, -(d/\tau\delta)\, e^{-\delta\eta}\right)}{\Gamma(c/\tau\delta, 0, -d/\tau\delta)}. \tag{30}$$

Here, it is important to refer to that at particular values for the physical parameters we can get two positive roots for (29); this leads to the dual solutions for the velocity and the temperature as clarified latter in the next section.

4. Results and Discussion

In the previous section the exact analytical solutions for the slip effect on the flow and heat transfer of nanofluids past a stretching sheet/shrinking sheet (with suction) have been calculated. The present paper is an extension of the study made by the author [10] in which the slip boundary condition and the shrinking case were not considered. Therefore, we aim in this section not only to compare the current results (when $\lambda = 0$) with those obtained in [10] at the same values of the physical parameters but also to study the effect of the slip parameter on the behaviour of the fluid velocity $f'(\eta)$ and the temperature distribution $\theta(\eta)$ in the case of shrinking sheet. For purpose of comparison, we present in Figure 1 the effect of the magnetic parameter M on the distribution of the velocity in the case of no slip, that is, at $\lambda = 0$. The results showed good agreement with those obtained by [10] (Figure 1).

Regarding the temperature distribution, the exact solution for $\theta(\eta)$ was obtained in [10] in the case of no slip in terms of the Whittaker M function and the hypergeometric function which are more complicated special functions than the generalized incomplete gamma function of the current analysis. It may be reasonable to refer here to that the analytical procedure followed in this paper is easier than the one considered in [10]. Figure 2 shows the effect of the magnetic parameter M on the temperature distribution in the case of no slip. The results also showed good agreement with those obtained by [10] (Figure 2). Although different

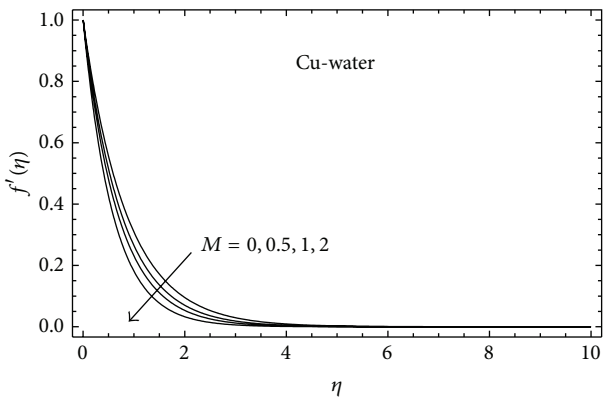

Figure 1: Effect of M on velocity distribution $f'(\eta)$ for Pr = 6.2 and $\phi = 0.1$.

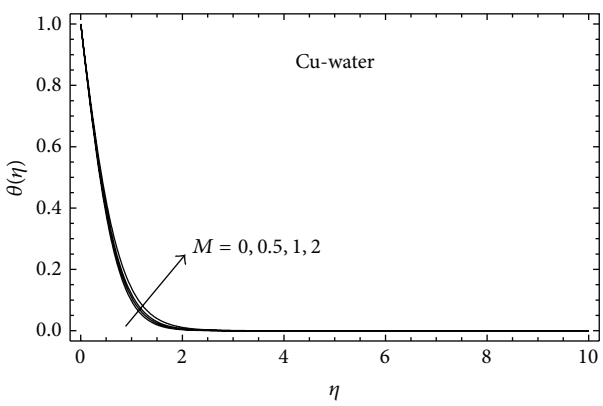

Figure 2: Effect of M on temperature distribution $\theta(\eta)$ for Pr = 6.2 and $\phi = 0.1$.

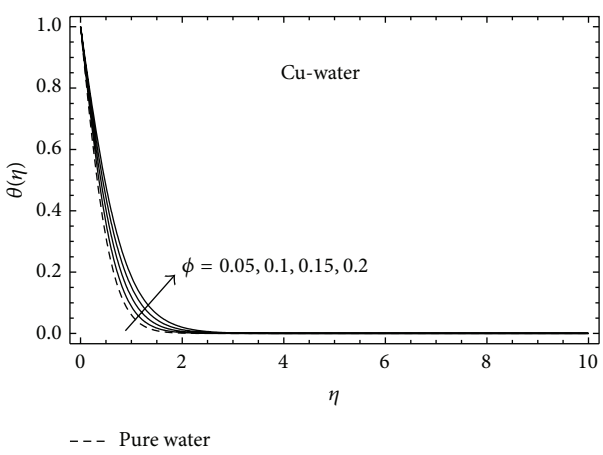

Figure 3: Effect of ϕ on temperature distribution $\theta(\eta)$ for Pr = 6.2 and $M = 1$.

special functions have been used in [10] to express $\theta(\eta)$, the same results have been obtained with the impression that our procedure is easier. In order to confirm this point additional plots are depicted in Figure 3 for the effect of the volume fraction of the Cu-nanoparticles on temperature distribution, where also good agreement has been achieved.

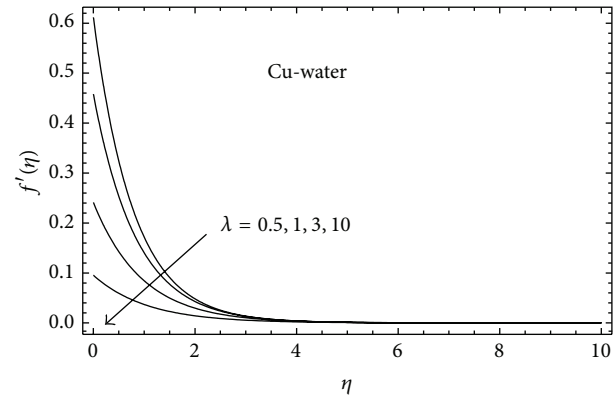

Figure 4: Effect of λ on velocity distribution $f'(\eta)$ for Pr = 6.2, $M = 1$, and $\phi = 0.1$.

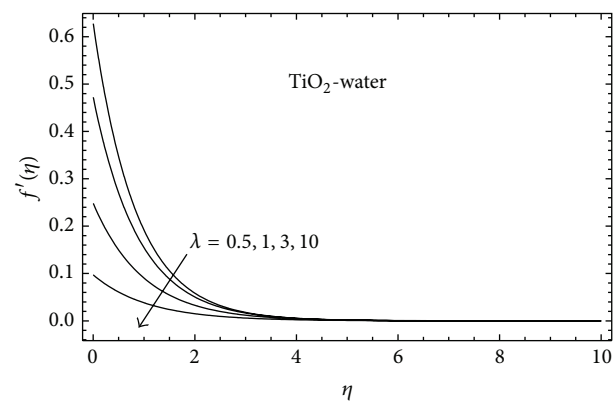

Figure 5: Effect of λ on velocity distribution $f'(\eta)$ for Pr = 6.2, $M = 1$, and $\phi = 0.1$.

The effect of the slip parameter λ on the velocity distribution $f'(\eta)$ is depicted in Figures 4 and 5 for the Cu-water and the TiO_2-water nanofluids, respectively, when Pr = 6.2 (water), $M = 1$, and $\phi = 0.1$. It is observed form these figures that the velocities of the Cu-water and the TiO_2-water nanofluids decrease with increasing the slip parameter. It seems from Figures 4 and 5 that the Cu-water and the TiO_2-water nanofluids have the same magnitude of velocity at all the values of the slip parameter. In order to declare this point, these two figures are collected in Figure 6 which shows that $f'(\eta)|_{\text{Cu-water}} < f'(\eta)|_{TiO_2\text{-water}}$ for the small values of the slip parameter, that is, $\lambda \leq 3$, while $f'(\eta)|_{\text{Cu-water}} \approx f'(\eta)|_{TiO_2\text{-water}}$ for the higher values of the slip parameter, that is, $\lambda > 3$. The results reveal that the Cu-water nanofluid is slower than the TiO_2-water nanofluid when the slip parameter is in the range $0 \leq \lambda \leq 3$; otherwise, the two nanofluids have the same magnitude of velocity. Figures 7 and 8 display the effect of the slip parameter on the temperature distribution of the Cu-water and the TiO_2-water nanofluids, respectively. It is clear from these figures that the temperature of the two nanofluids increases with the increase of the slip parameter. Figure 9 shows that the temperature of the Cu-water nanofluid is always higher than the temperature of the TiO_2-water nanofluid whatever the values of the slip parameter.

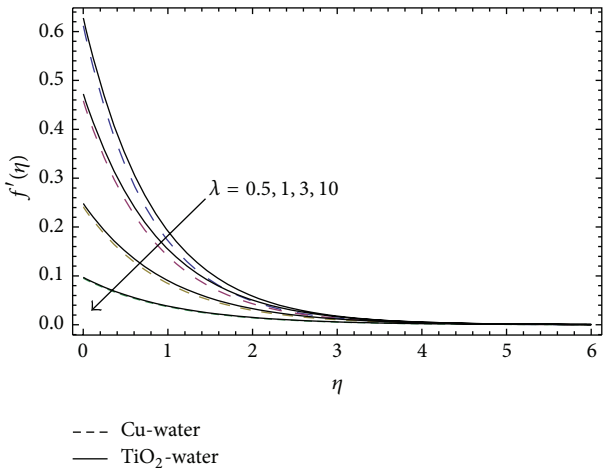

FIGURE 6: Effect of λ on the velocity distribution $f'(\eta)$ for the Cu-water and the TiO_2-water nanofluids at Pr = 6.2, $M = 1$, and $\phi = 0.1$.

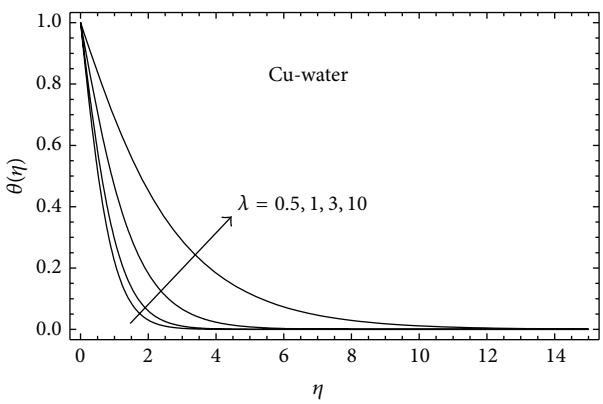

FIGURE 7: Effect of λ on temperature distribution $\theta(\eta)$ for Pr = 6.2 and $M = 1$.

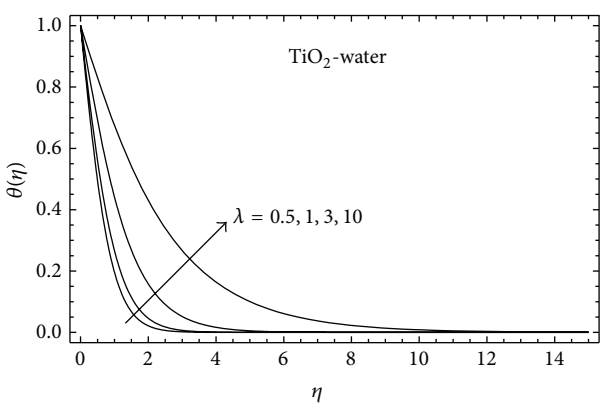

FIGURE 8: Effect of λ on temperature distribution $\theta(\eta)$ for Pr = 6.2 and $M = 1$.

In the case of the shrinking sheet it is has been shown in Figures 10 to 14 that dual solutions have been obtained for the velocity and the temperature at the indicated parameters. In Figure 10(a) the effect of the volume fraction of the Cu-nanoparticles on the dual velocity is plotted. For the upper solution branch it is shown that $f'(\eta)$ decreases with the

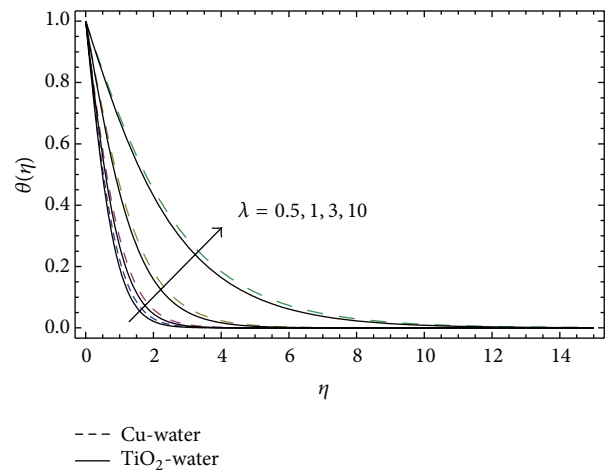

FIGURE 9: Effect of λ on the temperature distribution $\theta(\eta)$ for the Cu-water and the TiO_2-water nanofluids at Pr = 6.2, $M = 1$, and $\phi = 0.1$.

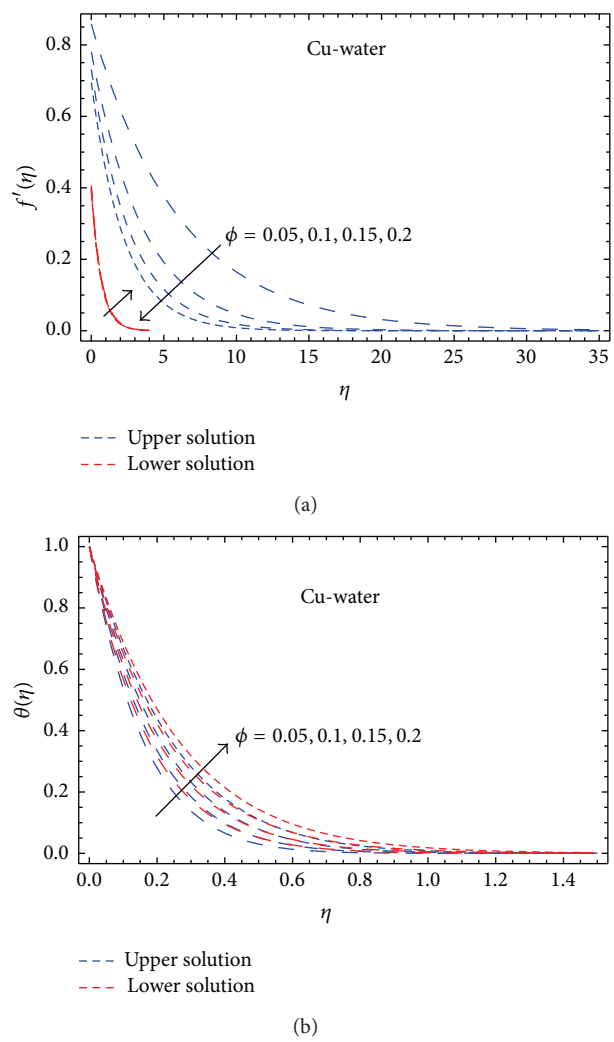

FIGURE 10: (a) Dual velocity for several values of ϕ at $s = 1$, $\lambda = 1$, and $M = 1$. (b) Dual temperature for several values of ϕ at $s = 1$, $\lambda = 1$, and $M = 1$.

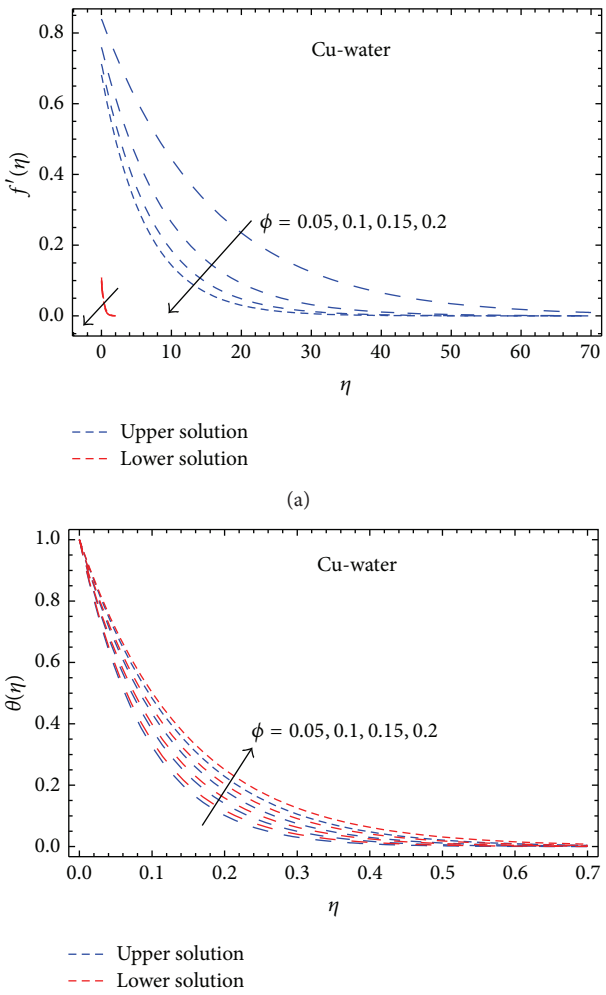

FIGURE 11: (a) Dual velocity for several values of ϕ at $s = 2$, $\lambda = 3$, and $M = 1$. (b) Dual temperature for several values of ϕ at $s = 2$, $\lambda = 3$, and $M = 1$.

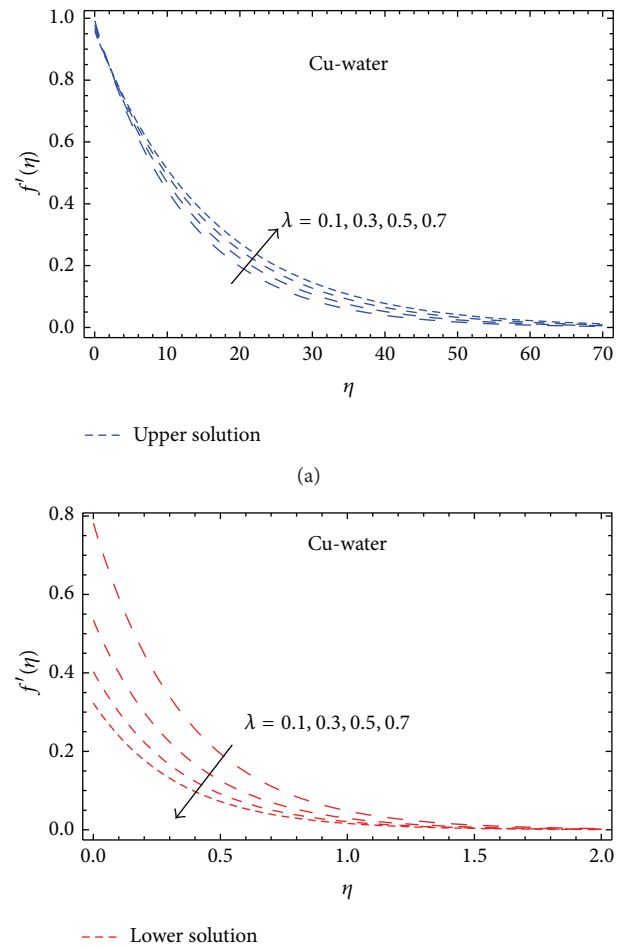

FIGURE 12: (a) Upper velocity solution for several values of λ at $s = 2$, $\phi = 0.1$, and $M = 1.5$. (b) Lower velocity solution for several values of λ at $s = 2$, $\phi = 0.1$, and $M = 1.5$.

increase of ϕ; however, a converse behaviour is observed for the lower solution branch of the velocity where slight increasing is observed. The situation for the effect of ϕ on the dual temperature is unique as depicted in Figure 10(b), where increasing ϕ increases the temperature for both the upper and the lower branches of the temperature. At different values of the selected parameters, it is shown in Figure 11(a) that both the upper and the lower branches of the dual velocity decreases with increasing the the volume fraction of the Cu-nanoparticles. However, the situation for the effect of ϕ on the dual temperature in Figure 11(b) is also unique and this agrees with the results obtained in Figure 10(b). The effect of the slip parameter λ on the dual velocity distributions $f'(\eta)$ is depicted in Figures 12(a) and 12(b) for the Cu-water nanofluid. For the upper solution there is an increase in the velocity with increasing the slip parameter, while a converse behaviour is found for the lower solution branch. Figure 13 shows the effect of the small values of the slip parameter on the variation of the dual temperature solutions. It may be concluded from Figure 13 that the small variation in λ has no effect on the variation of the temperature. The effect of such slip parameter at higher values on the dual solutions of both the Cu-water and the TiO_2-water nanofluids is depicted in Figures 14(a) and 14(b). The upper solution of both the two nanofluids increases with the increase of the slip parameter. For the lower solutions, the increase in the slip parameter decreases the velocities of the two nanofluids. One further observation here is that in the case of shrinking sheet the velocity of the Cu-water nanofluid is also slower than the TiO_2-water nanofluid and these results are similar to those obtained in the case of the stretching sheet.

5. Conclusion

The effect of the velocity slip boundary condition on the flow and heat transfer of Cu-water and TiO_2-water nanofluids in the presence of a magnetic field is investigated in this paper. The system of nonlinear differential equations governing the flow is exactly solved in terms of the exponential function

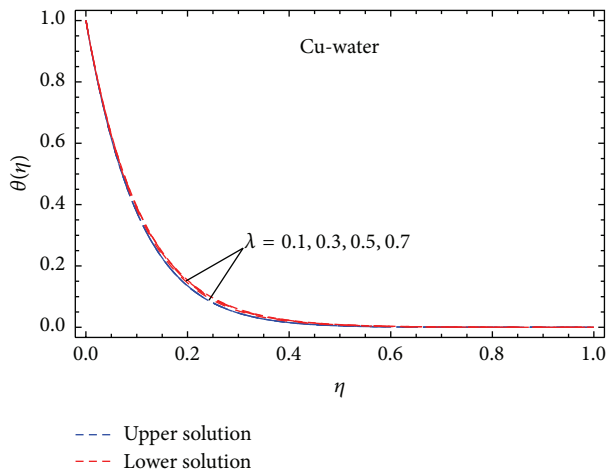

FIGURE 13: Dual temperature for several values of λ at $s = 2$, $\phi = 0.1$, and $M = 1.5$.

for the fluid velocity and in terms of the generalized incomplete gamma function for the temperature distribution. In comparison with the previously published results, an easier analytical procedure has been suggested in this work to obtain the exact solutions. The main results of the present paper can be summarized as follows.

(I) In the case of the stretching sheet,

(i) the velocities of the Cu-water and the TiO_2-water nanofluids decrease with increasing the slip parameter λ;

(ii) velocity$|_{\text{Cu-water}}$ < velocity$|_{TiO_2\text{-water}}$, for $\lambda \leq 3$, while velocity$|_{\text{Cu-water}} \approx$ velocity$|_{TiO_2\text{-water}}$, when $\lambda > 3$;

(iii) the Cu-water nanofluid is slower than the TiO_2-water nanofluid when the slip parameter is in the range $0 \leq \lambda \leq 3$; otherwise, the two nanofluids have the same magnitude of velocity;

(iv) the temperature of the two nanofluids increases with the increase of the slip parameter;

(v) the temperature of the Cu-water nanofluid is always higher than the temperature of the TiO_2-water nanofluid whatever the values of the slip parameter.

(II) In the case of the shrinking sheet,

(i) there are dual solutions for the velocity and the temperature at particular values of the physical parameters;

(ii) the Cu-water nanofluid is slower than the TiO_2-water nanofluid as in the case of the stretching sheet;

(iii) the effect of ϕ on the dual temperature is unique, where increasing ϕ increases the temperature for both the upper and the lower branches of the temperature.

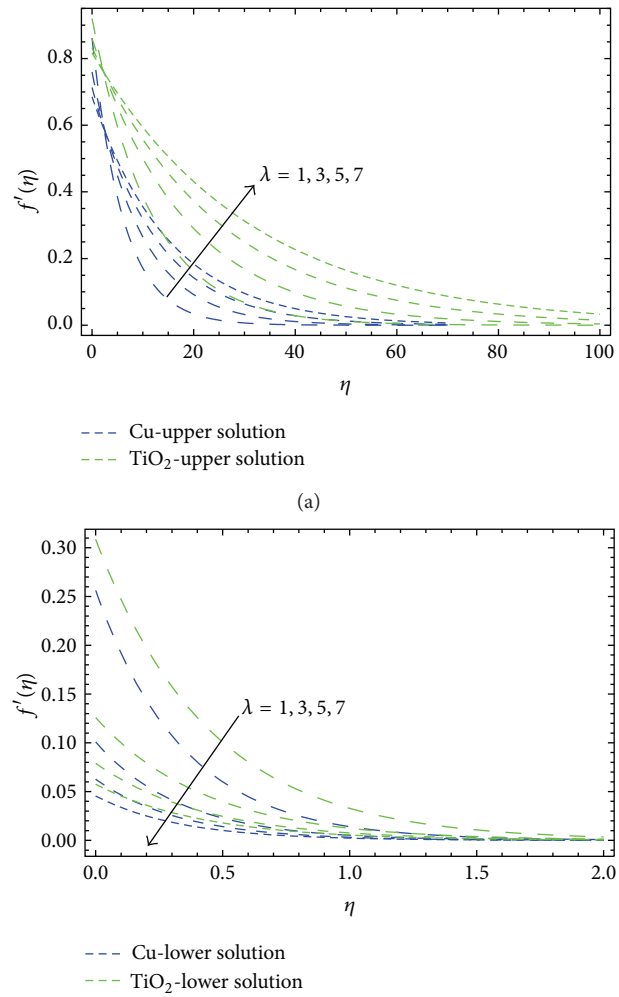

FIGURE 14: (a) Upper velocity solutions for several values of λ for the Cu-water and the TiO_2-water nanofluids at $s = 2$, $\phi = 0.1$, and $M = 1$. (b) Lower velocity solutions for several values of λ for the Cu-water and the TiO_2-water nanofluids at $s = 2$, $\phi = 0.1$, and $M = 1$.

Conflict of Interests

The authors declare that there is no conflict of interests regarding the publication of this paper.

Acknowledgment

The authors would like to acknowledge financial support for this work from the Deanship of Scientific Research (DSR), University of Tabuk, Tabuk, Saudi Arabia, under Grant no. S/105/1435.

References

[1] T. Metal, S. Oh, and H. Gegel, *Metal Forming Fundamentals and Applications*, American Society of Metals, Metals Park, Ohio, USA, 1979.

[2] M. V. Karwe and Y. Jaluria, "Numerical simulation of thermal transport associated with a continuously moving flat sheet in materials processing," *Journal of Heat Transfer*, vol. 113, no. 3, pp. 612–619, 1991.

[3] W. C. W. Chan, *Bio-Applications of Nanoparticles*, Springer Science, New York, NY, USA, 2007.

[4] S. U. S. Choi, "Enhancing thermal conductivity of fluids with nanoparticles," *Developments and Applications of Non-Newtonian Flows*, vol. 66, pp. 99–105, 1995.

[5] R. Saidur, K. Y. Leong, and H. A. Mohammad, "A review on applications and challenges of nanofluids," *Renewable and Sustainable Energy Reviews*, vol. 15, no. 3, pp. 1646–1668, 2011.

[6] X. Q. Wang and A. S. Mujumdar, "Heat transfer characteristics of nanofluids: a review," *International Journal of Thermal Sciences*, vol. 46, no. 1, pp. 1–19, 2007.

[7] X. Q. Wang and A. S. Mujumdar, "A review on nanofluids—part II: experiments and applications," *Brazilian Journal of Chemical Engineering*, vol. 25, no. 4, pp. 631–648, 2008.

[8] J. A. Eastman, S. U. S. Choi, S. Li, W. Yu, and L. J. Thompson, "Anomalously increased effective thermal conductivities of ethylene glycol-based nanofluids containing copper nanoparticles," *Applied Physics Letters*, vol. 78, no. 6, pp. 718–720, 2001.

[9] Y. Xuan and Q. Li, "Investigation on convective heat transfer and flow features of nanofluids," *Journal of Heat Transfer*, vol. 125, no. 1, pp. 151–155, 2003.

[10] M. A. A. Hamad, "Analytical solution of natural convection flow of a nanofluid over a linearly stretching sheet in the presence of magnetic field," *International Communications in Heat and Mass Transfer*, vol. 38, no. 4, pp. 487–492, 2011.

[11] A. Noghrehabadi, M. Ghalambaz, and M. Ghalambaz, "A theoretical investigation of SiO_2-water nanofluid heat transfer enhancement over an isothermal stretching sheet," *International Journal of Multidisciplinary Sciences and Engineering*, vol. 2, no. 9, pp. 18–21, 2011.

[12] A. Noghrehabadi, M. Ghalambaz, and A. Ghanbarzadeh, "Comparing thermal enhancement of Ag-water and SiO_2-water nanofluids over an isothermal stretching sheet with suction or injection," *Computer Methods in Applied Mechanics and Engineering*, vol. 2, no. 1, pp. 35–47, 2012.

[13] K. Vajravelu, K. V. Prasad, and C.-O. Ng, "The effect of variable viscosity on the flow and heat transfer of a viscous Ag-water and Cu-water nanofluids," *Journal of Hydrodynamics*, vol. 25, no. 1, pp. 1–9, 2013.

[14] N. L. Alegn, N. Bachok, and A. Ishak, "Effects of suction and injection on a moving plate in a nanofluid: Alumina-water," *AIP Conference Proceedings*, vol. 1522, pp. 405–412, 2013.

[15] K. Das, "Mixed convection stagnation point flow and heat transfer of Cu-water nanofluids towards a shrinking sheet," *Heat Transfer—Asian Research*, vol. 42, no. 3, pp. 230–242, 2013.

[16] E. H. Aly and A. Ebaid, "Exact analytical solution for suction and injection flow with thermal enhancement of five nanofluids over an isothermal stretching sheet with effect of the slip model: a comparative study," *Abstract and Applied Analysis*, vol. 2013, Article ID 721578, 14 pages, 2013.

[17] M. Majumder, N. Chopra, R. Andrews, and B. J. Hinds, "Nanoscale hydrodynamics: enhanced flow in carbon nanotubes," *Nature*, vol. 438, article 44, 2005.

[18] E. H. Aly, A. Ebaid, and N. Y. Abd Elazem, "Analytical and numerical investigations for the flow and heat transfer of nanofluids over a stretching sheet with partial slip boundary condition," *Applied Mathematics & Information Sciences*, vol. 8, no. 4, pp. 1639–1645, 2012.

[19] M. Gad-el-Hak, "The fluid mechanics of macrodevices-the Freeman scholar lecture," *Journal of Fluids Engineering*, vol. 121, pp. 5–33, 1999.

[20] R. A. van Gorder, E. Sweet, and K. Vajravelu, "Nano boundary layers over stretching surfaces," *Communications in Nonlinear Science and Numerical Simulation*, vol. 15, no. 6, pp. 1494–1500, 2010.

[21] H. F. Oztop and E. Abu-Nada, "Numerical study of natural convection in partially heated rectangular enclosures filled with nanofluids," *International Journal of Heat and Fluid Flow*, vol. 29, no. 5, pp. 1326–1336, 2008.

[22] K. Khanafer, K. Vafai, and M. Lightstone, "Buoyancy-driven heat transfer enhancement in a two-dimensional enclosure utilizing nanofluids," *International Journal of Heat and Mass Transfer*, vol. 46, no. 19, pp. 3639–3653, 2003.

[23] K. Khanafer and K. Vafai, "A critical synthesis of thermophysical characteristics of nanofluids," *International Journal of Heat and Mass Transfer*, vol. 54, no. 19-20, pp. 4410–4428, 2011.